Noise-Sustained Structure in Taylor-Couette Flow with Through Flow

Kenneth L. Babcock, Guenter Ahlers, and David S. Cannell
Department of Physics and Center for Nonlinear Science, University of California, Santa Barbara, California 93106
(Received 8 July 1991)

We report experimental and theoretical results for the absolute and convective instability boundaries in Taylor-Couette flow with imposed axial flow as a function of the axial Reynolds number. Experiment and theory agree quantitatively. In the downstream region of a large-aspect-ratio system, noise-sustained structures of traveling vortices exist in much of the convectively unstable regime. These structures have a nearly time-independent amplitude, but a noisy phase. The phase noise ceases abruptly upon crossing the absolute instability boundary.

PACS numbers: 47.20.−k, 43.50.+y, 47.25.Mr

The sensitivity of open flows to perturbations has been well documented since Leconte observed "musically inclined" jets responsive to acoustic excitation [1]. Numerous examples exist for open systems such as pipe and channel flows and obstacle wakes [2,3]. However, the role of noise in destabilizing laminar states and producing turbulence remains unclear.

In open systems it is important to distinguish between absolutely unstable flows, in which disturbances grow at any fixed point, and convectively unstable ones, in which fluctuations grow only in a comoving frame [4–6]. In the latter case, individual fluctuations grow as they are advected downstream, but are eventually "blown out" of the system so that no permanent structure is produced in the absence of noise or perturbations. However, in a study of a complex Ginzburg-Landau (CGL) equation which models many open flows, it was found that a weak but persistent noise source generated sustained structures in the downstream portion of the system [7].

In this Letter we describe an investigation of stability and noise in an open flow, namely, Taylor-Couette flow between concentric cylinders [8] with imposed axial flow. Experimentally we find that if the system is sufficiently long, noise-sustained structure predominates when the base flow is convectively unstable. The observed structures are patterns of traveling Taylor vortices whose phase varies irregularly with time. This irregularity vanishes within our resolution at the transition from convective to absolute instability. We presume that the patterns are sustained by noise originating in the inlet region. As shown below, noise effects can be observed near the onset of the centrifugal (Taylor) instability even at small axial Reynolds numbers $R \lesssim 4$. Our observations clarify the interplay between noise and stability, and permit a quantitative description by the appropriate CGL equation.

The experiments were performed in a modified Taylor-Couette apparatus with the inner cylinder rotating. A recirculating gravity feed generated axial flow whose rate was controlled to an accuracy of 0.2%. The radius ratio r_1/r_2 was 0.738 and the aspect ratio L/d was 144. Here $d = r_2 - r_1$ and the total length $L = 98$ cm. Both cylinders were concentric and straight to ± 0.04 mm. We used water-glycerol mixtures seeded with 1% Kalliroscope suspension by volume for flow visualization. A computer-interfaced charge-coupled-device camera recorded scan lines and time series of reflected light. The fluid temperature was controlled to better than ± 30 mK. Before entering the gap, the fluid passed through an annulus containing eight holes of diameter 1.1 mm, followed by two layers of 0.44-mm-mesh stainless-steel screen to produce azimuthally uniform axial flow.

This system has two control parameters. One is the axial Reynolds number $R \equiv \langle w \rangle d/\nu$, where $\langle w \rangle$ is the mean axial flow velocity and ν the kinematic viscosity. The second is the reduced angular rotation frequency of the inner cylinder $\epsilon \equiv \omega/\omega_0 - 1$, where ω_0 refers to the onset of Taylor-vortex flow at $R = 0$ [8]. The structureless base flow, comprised of circular Couette flow superimposed with axial Poiseuille flow, first becomes unstable to traveling vortices [9]. Recently, the distinction between convective and absolute instability has been examined for this system [10] and for thermal convection with through flow [11]. Below we describe high-resolution measurements of the convective and absolute instability regimes made possible by the long aspect ratio of our apparatus.

We found that convective instability could be directly observed by generating localized perturbations in the base flow at fixed ϵ and R. This was done by rotating both cylinders about their axis back and forth once through a small angle [12]. As shown in the space-time plot of Fig. 1, a pulse localized to within two or three vortex pairs appeared at the inlet and traveled into the system. The pulse initially decayed over a fraction of the distance $\langle w \rangle d^2/\nu$, which is approximately that required for the inlet flow to attain the angular momentum of the base flow. The pulse then spread, grew in amplitude, and was advected out of the system. To probe the onset of convective instability, time series of reflected light were recorded as pulses passed a point $100d$ from the inlet. The amplitude of the fundamental peak in the discrete Fourier transform (DFT) was found for pulses at various ϵ for given R. Reducing ϵ caused slower pulse growth, and hence weaker signals at the observation point. The intersection of the DFT peak amplitude with the noise base line was taken as the onset of convective instability ϵ_c. Figure 2 shows the results for $R \lesssim 20$. At larger R, spiral modes [13] grew and complicated the measurements.

We also calculated numerically the onset of convective

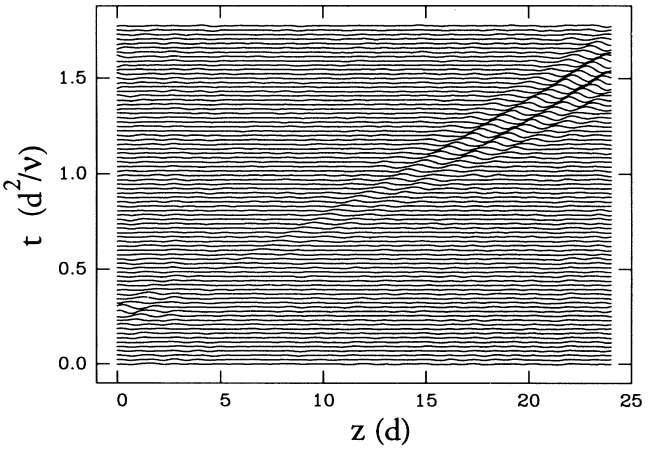

FIG. 1. Pulse growth in the convectively unstable regime; $R=16.5$ and $\epsilon=0.160$. At time $t=0.2$, the apparatus was rocked back and forth once. The length shown is about $L/6$.

instability for our experimental geometry from the Navier-Stokes equations. Instability to modes of the form $\exp[i(kz-\Omega t+m\Theta)]$ was examined, where t is the time, and z and Θ are the axial and azimuthal coordinates, respectively. For axisymmetric modes ($m=0$), the results are well fitted by $\epsilon_c=0.000381R^2(1-9.3\times10^{-5}R^2)$, shown as the solid curve in Fig. 2. They are in excellent agreement with our measurements [14], and are consistent with previous calculations for other radius ratios [13].

For ϵ sufficiently greater than ϵ_c, structure was observed in the absence of applied perturbations. Figure 3 shows space-time plots of traveling vortex patterns at several ϵ for $R=3.0$. The pattern amplitude was roughly time independent at a given position, but decreased to zero, or nearly zero, at the inlet because the flow entered with no azimuthal velocity. The spatial growth may be measured by the healing length l_h at which the pattern reaches half its maximum amplitude [11]. As can be seen in Fig. 3, l_h grew and the amplitude of the pattern at

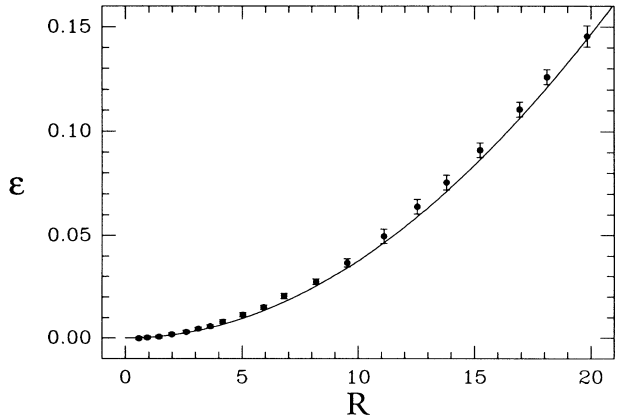

FIG. 2. Convective instability boundary ϵ_c obtained by observing pulse growth. The curve is the linear stability result.

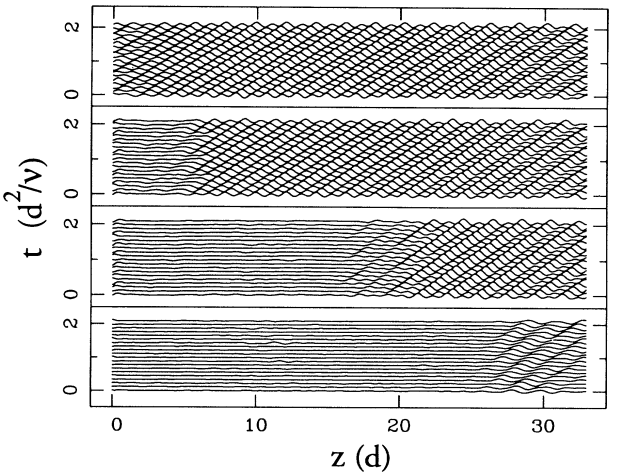

FIG. 3. Space-time plots of patterns at $R=3.0$, showing the increase in healing length l_h as ϵ decreases. Top to bottom: $\epsilon=0.1020$, 0.0822, 0.0632, and 0.0347. About $\frac{1}{4}$ of the apparatus is shown.

large z decreased as ϵ was reduced.

A recent numerical study of thermal convection with through flow found that, in the absence of noise, patterns resembling those in Fig. 3 arose only in the absolutely unstable regime [11]. The healing length l_h increased as ϵ was reduced, and diverged at the boundary ϵ_a between convective and absolute instability. However, as suggested by the CGL equation [7], one expects that noise-sustained structure with finite l_h can exist in the convectively unstable regimes of real systems. We shall see that the lower two plots in Fig. 3 are examples of such structures. A diagnostic other than the behavior of l_h is thus necessary to locate ϵ_a in the presence of noise.

Detailed examination of the structures of Fig. 3 revealed a qualitative change as ϵ was reduced. After

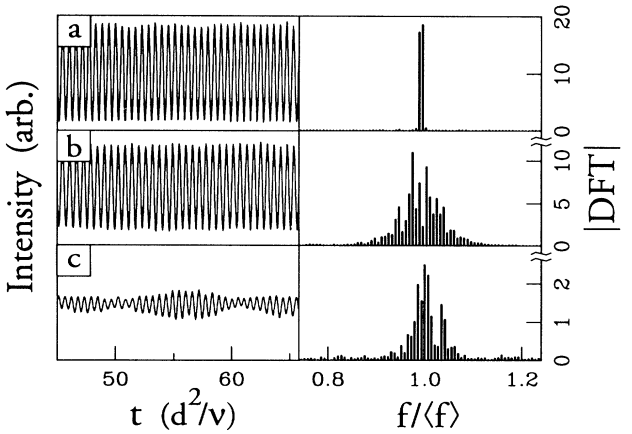

FIG. 4. Time series, and DFT moduli near the fundamental peak, at $z=100d$ for $R=3.0$. About $\frac{1}{4}$ of each series is shown. (a) $\epsilon-\epsilon_c=0.0896$. (b) $\epsilon-\epsilon_c=0.0318$. The DFT peak shows considerable broadening. In (c), structure persists at small $\epsilon-\epsilon_c=0.0077$.

fixing ϵ and R and waiting for transients to die away, time series of reflected light were recorded for $z=100d$. Figure 4 shows portions of time series and corresponding DFT moduli for various ϵ at $R=3.0$. Each series covered about 160 periods and contained 2048 points. In Fig. 4(a), $\epsilon-\epsilon_c=0.0896$, and the data appear periodic and of nearly uniform amplitude. The corresponding fundamental DFT peak is very sharp. At $\epsilon-\epsilon_c=0.0318$ in Fig. 4(b), the time series remains fairly uniform in amplitude, but the DFT peak has become much broader. Demodulation shows that this broadening is due to irregular time dependence of the phase. As shown for $\epsilon-\epsilon_c=0.0077$ in Fig. 4(c), sustained patterns persist to small $\epsilon-\epsilon_c$, but the amplitude shows time variation, and the DFT remains broad. The transition in spectral width can be characterized by the normalized variance of the fundamental peak in the power spectrum $\sigma^2=\langle(f-\langle f\rangle)^2\rangle/\langle f\rangle^2$, calculated by integrating over frequencies in the vicinity of the fundamental component. The experimental result for a range of ϵ at $R=3.0$ is shown in Fig. 5(a). The sharp increase in σ^2 below $\epsilon=0.065$ corresponds to the onset of phase noise.

Simulations of the CGL equation

$$\tau_0(\dot{A}+sA')=\tilde{\epsilon}(1+ic_0)A+\xi_0^2(1+ic_1)A''-g(1+ic_2)|A|^2A \quad (1)$$

showed that the transition in $\sigma^2(\epsilon)$ is related to the boundary dividing absolute and convective instability. Equation (1) is derived from an expansion around ϵ_c. Here $\tilde{\epsilon}=\omega/\omega_c(R)-1=(\epsilon-\epsilon_c)/(1+\epsilon_c)$, and $s\propto R$ is the group velocity of the critical mode at onset. Length and time are scaled by the gap d and diffusion time d^2/ν, respectively. For the linear terms, coefficients specific to our geometry were obtained from the stability analysis described above [15]. A discrete version of Eq. (1) was numerically integrated. Noise was modeled by choosing random values for the real and imaginary parts of $A(z=0)$ at each time step, a form chosen because the most relevant noise originates in the inlet region. Values were uniformly distributed between $\pm n$, where we call n the noise level. We mimicked the experiment by analyzing time series of the function $\Psi=\mathrm{Re}\{A(z,t)\exp[i(k_cz-\Omega_ct)]\}$ at $z=100d$. The time series and their DFTs closely resembled their experimental counterparts. As shown in Fig. 5(b), the peak variance σ^2 undergoes a transition remarkably similar to that in the experiment. Demodulation shows that the broadening is again due to phase noise.

It is readily shown [7,11] that the boundary between convective and absolute instability in Eq. (1) occurs at $\tilde{\epsilon}_a^{\mathrm{CGL}}=(s\tau_0/2\xi_0)^2/(1+c_1^2)$. The vertical dashed line in Fig. 5(b) corresponds to $\tilde{\epsilon}_a^{\mathrm{CGL}}$ for our geometry at $R=3.0$. The onset of phase noise is clearly identified with $\tilde{\epsilon}_a^{\mathrm{CGL}}$ and is also insensitive to the noise level. The onset varied less than $\delta\epsilon=\pm0.005$ for $10^{-9}\le n\le10^{-3}$, where onset is taken to be the point where the variance σ^2 first departs from the base line. Thus, even though the physical noise source and level are uncertain, we are confident that the experimental transition to phase noise corresponds to the boundary ϵ_a.

Figure 6 shows the complete stability diagram for axisymmetric patterns up to $R\simeq4.0$. The upper data points mark ϵ_a, identified by the transition to phase noise. For $R\gtrsim4$, spiral modes grew and interfered with measurements of ϵ_a. We calculated the absolute stability boundary from the full equations [16], using methods outlined in Refs. [5] and [6]. The results are well fitted by $\epsilon_a=0.00782R^2(1-0.0043R^2)$, and are shown as the upper

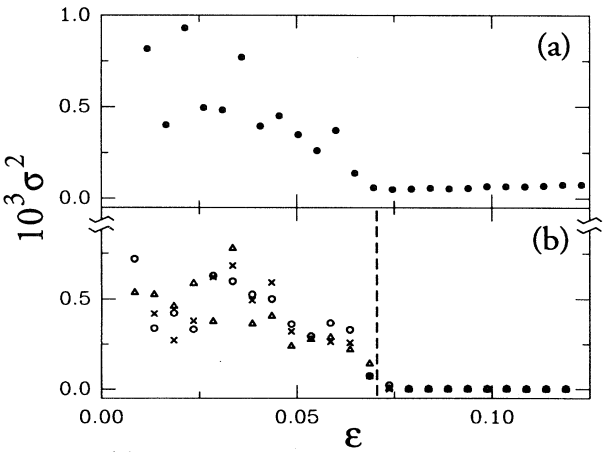

FIG. 5. (a) Normalized variance of the fundamental peak in the DFT power vs ϵ at $R=3.0$ for time series at $z=100d$. The transition at $\epsilon=0.065$ indicates the onset of phase noise. (b) Corresponding results for Eq. (1) for noise levels 10^{-6} (×), 10^{-5} (△), and 10^{-4} (○), respectively. The dashed line locates $\epsilon_a^{\mathrm{CGL}}=0.071$.

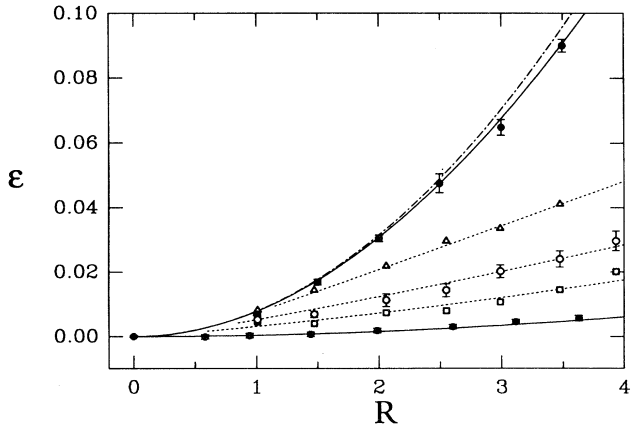

FIG. 6. Stability diagram for axisymmetric structures. The lower points and solid curve are for the onset of convective instability. The upper data points locate the experimental transition to phase noise, the upper solid curve is the linear stability result for ϵ_a, and the dash-dotted line is $\epsilon_a^{\mathrm{CGL}}$. Open symbols indicate the boundary ϵ_s for noise-sustained structure at $z=25d$ (△), $z=50d$ (○), and $z=100d$ (□). The dotted lines are the estimates of ϵ_s given by Eq. (2) with $A_{\min}/A_0^{\mathrm{fr}}=590$.

solid curve. The lower set of data points is for the convective instability boundary ϵ_c, and the corresponding solid curve is the linear stability result. Experiment and theory agree very well for both boundaries. The upper dash-dotted curve is the CGL result $\epsilon_a^{\mathrm{CGL}}=0.00789R^2(1-0.0008R^2)$. Its close agreement with the experiment and the full equations suggests that Eq. (1) applies rather well throughout the parameter range of Fig. 6.

With the stability boundaries precisely located, we can be sure that structures observed at $\epsilon<\epsilon_a$, such as the lower two plots of Fig. 3, are sustained by noise. We measured ϵ_s, the minimum ϵ for which structure was observed, at various distances from the inlet. A spectral method similar to that employed in measuring the convective instability boundary was used. The results for $z=25d$, $50d$, and $100d$ are shown in Fig. 6 as open symbols. Further from the inlet, structure was observed at increasingly smaller ϵ, because fluctuations had more time to grow. In the limit of very large aspect ratio, the boundary ϵ_s approaches ϵ_c, and noise-sustained structure predominates in the convectively unstable regime [17].

The effects of noise can be modeled by an effective inlet boundary condition $A_0^{\mathrm{eff}}\neq 0$ which gives rise to a time-independent amplitude

$$A(z)=A_0^{\mathrm{eff}}\exp\{z\tilde{\epsilon}_a^{1/2}[1-(1-\tilde{\epsilon}/\tilde{\epsilon}_a)^{1/2}]/\xi_0\} \qquad (2)$$

obtained as the solution of the linear part of Eq. (1). We may invert this expression for $\tilde{\epsilon}$ to give $\epsilon=\epsilon_c+(1+\epsilon_c)\tilde{\epsilon}$. After inserting the linear stability values for ϵ_c, ϵ_a, and ξ_0, this provides an estimate of the structure boundary ϵ_s with the single free parameter $A_{\mathrm{min}}/A_0^{\mathrm{eff}}$. Here A_{min} is the minimum experimentally detectable amplitude which prevails at ϵ_s. A fit to the data gives $A_{\mathrm{min}}/A_0^{\mathrm{eff}}\simeq 600$. The corresponding estimate of ϵ_s is shown as the dashed lines in Fig. 6. The estimate $A_{\mathrm{min}}=10^{-3}$ determined in a similar experimental configuration [18,19] yields $A_0^{\mathrm{eff}}\simeq 2\times 10^{-6}$. From simulations of Eq. (1), we find that a noise level about an order of magnitude larger than A_0^{eff}, or $n\simeq 2\times 10^{-5}$, produces amplitude profiles that match the data. These values motivated the choice of noise levels shown in Fig. 5(b).

In conclusion, we have shown that noise-sustained structure predominates in a convectively unstable open flow. The increase in phase noise at the transition from absolute to convective instability may serve as a useful diagnostic in other open flows (for example, object wakes [5]) which possess both instability regimes.

This work was supported by NSF Grant No. DMR 88-14485. It is a pleasure to thank Hanns Walter Müller, Steven Trainoff, and Morten Tveitereid for helpful discussions. We also thank Manfred Lücke for suggestions on estimating the effective noise strength.

[1] J. Leconte, Philos. Mag. **15**, 235 (1858).

[2] D. J. Tritton, *Physical Fluid Dynamics* (Oxford Univ. Press, Oxford, 1988), 2nd ed.

[3] M. F. Schatz, R. P. Tagg, H. L. Swinney, P. F. Fischer, and A. T. Patera, Phys. Rev. Lett. **66**, 1579 (1991).

[4] L. D. Landau and E. M. Lifshitz, *Fluid Mechanics* (Pergamon, New York, 1959), 1st ed.

[5] For a recent overview, see P. A. Monkewitz, Europhys. J. Mech. B **9**, 395 (1990), and references therein.

[6] Convective versus absolute instability in the closed Taylor-Couette system (i.e., without through flow) has been examined for the case of counterrotating cylinders by R. Tagg, W. S. Edwards, and H. L. Swinney, Phys. Rev. A **42**, 831 (1990).

[7] R. J. Deissler, J. Stat. Phys. **40**, 371 (1985); Physica (Amsterdam) **25D**, 233 (1987).

[8] A review of Taylor-Couette without through flow is given by R. C. DiPrima and H. L. Swinney, in *Hydrodynamic Instabilities and Transitions to Turbulence,* edited by H. L. Swinney and J. P. Gollub (Springer, Berlin, 1981).

[9] R. C. DiPrima, J. Fluid Mech. **9**, 621 (1960); R. J. Donnelly and D. Fultz, Proc. Natl. Acad. Sci., Wash. **46**, 1150 (1960); S. Chandrasekhar, Proc. R. Soc. London A **265**, 188 (1962); H. A. Snyder, Proc. R. Soc. London A **265**, 198 (1962).

[10] A. Tsameret and V. Steinberg, Europhys. Lett. **14**, 331 (1991).

[11] H. W. Müller, M. Lücke, and M. Kamps. Europhys. Lett. **10**, 451 (1989).

[12] Reproducible disturbances were created with a stepper motor linked to the outer cylinder. We typically rotated the apparatus by 1° during 0.1 s and paused 1.0 s before reversing direction.

[13] D. I. Takeuchi and D. F. Jankowski, J. Fluid Mech. **102**, 101 (1981); B. S. Ng and E. R. Turner, Proc. R. Soc. London A **382**, 83 (1982).

[14] The experiment of Ref. [10] used a different method in an apparatus of radius ratio $r_1/r_2=0.707$ and aspect ratio 27, and yielded $\epsilon_c\simeq 0.0016R^2$, about 4 times greater than our result.

[15] We found

$$k_c=3.136+0.000104R^2(1-0.00014R^2),$$
$$\Omega_c=3.677R(1+0.000020R^2),$$
$$\tau_0=0.0379-0.000024R^2(1-0.00046R^2),$$
$$s=1.230R(1+0.0000041R^2),$$
$$\xi_0^2=0.0725-0.000048R^2(1-0.00053R^2),$$
$$c_0=0.00720R(1-0.00038R^2),$$
$$c_1=0.0235R(1+0.00026R^2).$$

The amplitude scale was set by a nonlinear coefficient g of order 1. We used $c_2=0.0113R$ as in Ref. [11] for convection with through flow. Our results were insensitive to the particular (small) value of c_2.

[16] The absolute instability is governed by a saddle point in the dispersion relation allowing for complex frequency *and* wave number. See Refs. [5] and [6].

[17] In the experiment of Ref. [10], it was stated that no sustained structure was observed in the convectively unstable regime. That work used an aspect ratio $L/d=27$ and attempted to measure ϵ_a by finding a divergence in the healing length l_h. The result deviated from the CGL value for $R>1.3$. Note that our data for ϵ_s at $z=25d$ in Fig. 6 intersects ϵ_a near $R=1.2$, suggesting that the deviation in Ref. [10] was due to noise-sustained structure with a comparable noise level.

[18] M. A. Dominguez-Lerma, D. S. Cannell, and G. Ahlers, Phys. Rev. A **34**, 4956 (1986).

[19] The amplitude scale is set by the value $g=1.0$, as used in Ref. [18].